HEFAT2012
9th International Conference on Heat Transfer, Fluid Mechanics and Thermodynamics
16 – 18 July 2012
Malta

IMPACT OF COOLING CHANNEL GEOMETRY ON THERMAL MANAGEMENT AND PERFORMANCE OF A PROTON EXCHANGE MEMBRANE FUEL CELL

S. O. Obayopo, T. Bello-Ochende* and J. P. Meyer
Department of Mechanical and Aeronautical Engineering,
University of Pretoria,
Pretoria 0002,
South Africa.

E-mail: Tunde.Bello-Ochende@up.ac.za

ABSTRACT

Proton exchange membrane fuel cell has many distinctive features that made it an attractive alternative clean energy source, including low start-up, high power density, high efficiency, portability and remote applications. Commercial application of this energy source had been greatly hindered by series of technical issues ranging from inadequate water and heat management, intolerance to impurities such as CO, slow electrochemical kinetics at electrodes, and relatively high cost. An approach to stem the thermal build-up within the fuel cell structure that could lead to degradation of the system components is by integrating cooling channels as part of flow structure of the PEM fuel cell system. In this study, a numerical investigation was carried out to investigate the impact of cooling channel geometry in combination with temperature dependent operating parameters on thermal management and overall performance of a PEM fuel cell system. The evaluation is performed using a CFD code based on a finite volume approach. The systems net power and polarization curves are presented as a function of the system temperature, operating parameters and geometry. In addition, the parameters studied were optimized using a mathematical optimization code integrated with the commercial computational fluid dynamics code.

INTRODUCTION

A proton exchange membrane fuel cell (PEMFC) using hydrogen is one of the emerging fuel cells with many advantages ranging from emission of water as waste, operation at low temperature for quick start-up, and use of solid polymer as electrolytes, reducing both construction and safety complications. This fuel cell type is being highly considered as an alternative power source for stationary and mobile applications though with several technical challenges [1]. Operating temperatures of the fuel cell systems affects the maximum theoretical voltage at which a fuel cell can operate. Higher operating temperatures correspond to lower theoretical maximum voltages and lower theoretical efficiency. Though, higher temperature at the fuel cell electrodes increases electrochemical activity, which in turn increases efficiency [2]. Most current proton exchange membrane (PEM) fuel cells operate at low temperatures (<80 ^{o}C) encountering several performance difficulties especially in vehicular applications, such as reduced electrochemical kinetics at electrode sites, flooding (due to two-phase flows emergence), intolerance to impurities such as CO, insufficient heat rejection capability and relatively high cost. A recent approach is to operate this class of fuel cell at higher temperature (>100 ^{o}C) which eliminates some of these obstacles [3-6]. Operating PEM fuel cell at higher temperatures increases the reaction rates at both electrodes and consequently increases system efficiency. The quality of waste heat from the fuel cell stack which could be used in other system components requiring heat or used to run an additional thermodynamic heat for additional power is also enhanced at higher operating temperature. Also, there is a substantial reduction in incidence of water "flooding" that restricts oxygen transport by blocking the channel path and pores of the gas diffusion electrodes when fuel cell is operated at higher temperature. Temperature distribution in fuel cell is usually non-uniform even when there is constant mass flow rate in the flow channels [7]. This is primarily as a result of the heat transfer and phase changes in PEM fuel cells. This usually causes temperature fluctuations within the fuel cell system structure and affects the fuel cell performance. In order to alleviate the excessive temperature build-up in a PEM fuel cell, the heat generated by various processes in the fuel cell structure should be properly removed. Thermal management still remains a critical issue that need be resolved in order for PEM fuel cell technology to be feasible for various commercial

applications [8,9]. A number of numerical modelling studies have been reported in the literature to investigate heat/mass transfer in PEM fuel cell.

Yu *et al.* [10] investigated the performance of the Ballard PEM fuel cell in terms of electrochemical characteristics and water management. The study shows that the more the water supplied to the anode from its inlet, the higher the voltage, and usually the lower the anode exit temperature.

Coppo *et al.* [11] presented a 3-D model to study the influence of temperature on PEM fuel cell operation including two-phase flow in the gas distribution channel. The result obtained indicate that both liquid water transport within the gas diffusion layer (GDL) and liquid water removal from the surface of the GDL play an important role at determining variations in cell performance with temperature.

A 1-D non-isothermal model to analyse the effect of anode and cathode side temperatures on the membrane water distribution was presented by Yan *et al.* [12]. Their results shows that increasing the temperature on the anode side can lead to membrane dehydration and operating the fuel cell at high current density leads to membrane dehydration on the anode side due to strong electro-osmotic water drag at high current density.

Shimpalee and Dutta [13] conducted a 3-D non-isothermal numerical analysis with two-phase flow. The effect of heat produced by the electrochemical reaction and phase change of water on the cell performance was critically studied. Their study shows that inclusion of heat transfer in the fuel cell model shows degradation in the fuel cell performance. Their study underlines the importance of incorporating heat transfer aspect in fuel cell modelling.

Recently, Obayopo *et al.* [14] presented a 3-D numerical model to investigate effect of a range of operating conditions such as reactant flow rates, GDL porosity, channel geometry and flow orientation on the performance of a single PEM fuel cell and also to determine the optimal operating conditions. One of the important outcomes of their study is that fuel cell performance increases with increase in temperature from 60 to 80 ^{o}C for the model studied. Increasing the cell temperature beyond 80 ^{o}C result in higher levels of water loss in the cell until a critical temperature is attained where the evaporated water is greater than the amount of water being generated in the cell thereby resulting in total dry-out of the membrane.

Ju *et al.* [15] presented a 3-D non-isothermal, single-phase model for all the seven layers of the PEM fuel cell that accounts for various location-specific heat-generation mechanisms, including irreversible heating due to electrochemical reactions, heating due to entropy, and Joule (ohmic) heating due to membrane ionic resistance. They observed that the thermal effect on PEM fuel cells becomes more critical at higher cell current density and/or lower gas diffusion layer thermal conductivity. Their result further shows that temperature increase in the membrane is highly dependent on the GDL thermal conductivity and inlet humidity conditions.

A number of modelling approaches has been developed in the literature to predict thermal effect in PEM fuel cell as described above [10-15]. These represent a significant contribution in fuel cell thermal modelling, however, there are few reports on thermal cooling approaches to enhance thermal management in PEM fuel cell structure. Also, most models on thermal management in PEM fuel cell are aimed at gaining understanding and improving the kinetic process for thermal prediction and at improving individual fuel cell model performance. They do not address practical approach to reducing the incident temperature generated in the fuel cell structure.

One of the enhancement techniques to reduce the excessive temperature build-up in a PEM fuel cell is by using air/water (depending on fuel cell size) cooling conveyed through cooling channels as an integral part of the fuel cell flow structure. To the author's knowledge, studies on the impact of cooling channel geometric configuration on effective thermal heat transfer and performance in the fuel cell system are still limited in the literature, in particular, models that gives room for operating low temperature PEM fuel cell beyond the critical i.e. ≤ 80 ^{0}C [14] to intermediate high temperatures i.e. 100 – 150 ^{0}C without the need for special compatible high temperature resistant materials which are costly. This paper presents a numerical modelling study that investigates the geometrical effect of cooling channels in combination with the fuel cell stoichiometry ratio and relative humidity on thermal performance of PEM fuel cell. In addition, a mathematical optimisation tool is used to select the best geometric configuration (in relation to these fuel cell temperature dependent operating parameters) that improves cooling and enhance fuel cell performance. The results of this study will be of fundamental and practical interest to fuel cell engineers at improving thermal management and overall enhancement of PEM system performance.

Nomenclature

A	[m^2]	Channel cross-sectional flow area
C_k	[kg kg^{-1}]	mass fraction of chemical species
C_p	[J kg^{-1} K^{-1}]	Constant-pressure heat capacity
D_i^{eff}	[m^2 s^{-1}]	effective diffusion coefficient of species *i*
E_{OCV}	[V]	open circuit voltage
F	[$Cmol^{-1}$]	Faraday constant (96,487 C mol^{-1})
I	[Acm^{-2}]	exchange current density
i_o	[Acm^{-2}]	local current density
k^{eff}	[W m^{-1} K^{-1}]	effective thermal conductivity
M	[kg/s]	Channel mass flow rate
n		electron number
p	[Pa]	pressure
R	[mol^{-1} K^{-1}]	universal gas constant (8.314J mol^{-1} K^{-1})
Re		Reynolds number
S		source term
T	[K]	temperature
V	[V]	cell voltage

Greek symbols

Δ		difference operator
α_{an}		electrical transfer coefficient (anode)
α_{cat}		electrical transfer coefficient (cathode)
μ	[kg m^{-1} s^{-1}]	fluid viscosity
ε		porosity of porous media
μ	[kg/m.s]	Dynamic viscosity
η	[V]	overpotential
κ^{eff}	[kg s m^{-2}]	Effective dynamic viscosity
Φ	[V]	phase potential function
ρ	[kg m^{-3}]	density

Subscripts and superscripts

an	anode
cat	cathode
e	electrolyte
Eff	effective
k	species
opt	optimum
s	electronic conductive solid matrix
U	momentum
CO	Carbon oxide
CFD	computational fluid dynamics
GDL	gas diffusion layer
PEM	proton exchange membrane
PEMFC	proton exchange membrane fuel cell

MODEL DESCRIPTION

In the present study, numerical study and optimisation of geometric parameters of the cooling channel of a PEM fuel cell based on a three-dimensional full cell model is attempted and the impact on the cell performance is explored. The single-cell PEMFC consists of the anode flow channel, anode diffusion layer, MEA assembly, cathode diffusion layer, cathode flow channel, as well as array of cooling channels on the carbon plates. Fig. 1 shows the 3-D schematic of the model of the PEM fuel cell system. The influential factors considered in the study that could affect the fuel cell thermal behaviour and subsequently its performances are the stoichiometry ratio, relative humidity (RH), aspect ratio of cooling channels. Therefore, these influential parameters are selected as the design parameters to be optimised in this study. The main objective of the optimisation is to achieve the best PEM fuel cell performance in term of optimal current density (the objective function) at prescribed operating conditions. The other geometric and physicochemical properties for the fuel cell system are kept constant in this study and given in Table 1. As shown in Fig. 1, the cooling channels are within the bipolar plates and are separate from the species channels. Construct of the three (3) rectangular cooling channels transversely placed at equal distances at each side (anode and cathode) of the fuel cell are also shown in figure.

Table 1. Physicochemical properties of the modeled fuel cell

Description	Value
Cell operating temperature (^oC)	70
Air-side/fuel-side inlet pressure (atm)	3/3
Open-circuit voltage (V)	0.95
Porosity of gas diffuser layer	0.5
Permeability of gas diffuser layer (m^2)	1.76 x 10^{-11}
Tortuosity of gas diffuser layer	1.5
Porosity of catalyst layer	0.5
Permeability of catalyst layer (m^2)	1.76 x 10^{-11}
Tortuosity of catalyst layer	1.5
Porosity of membrane	0.28
Permeability of membrane (m^2)	1.8 x 10^{-18}
Reference diffusivity of H_2	11 x 10^{-5} m^2 s^{-1}
Reference diffusivity of O_2	3.2 x 10^{-5} m^2 s^{-1}
Electric conductivity of catalyst layer ($\Omega^{-1}m^{-1}$)	190
Electric conductivity of GDL ($\Omega^{-1}m^{-1}$)	300
Electric conductivity in carbon plate ($\Omega^{-1}m^{-1}$)	4000
O_2 stochiometry ratio	1.2
H_2 stochiometry ratio	2.0
Oxygen mole fraction	0.406
Relative humidity of inlet fuel/air	100%
Reference current density of anode	7 500
Reference current density of cathode (A/m^2)	20
Anode transfer coefficient	2.0
Cathode transfer coefficient	2.0

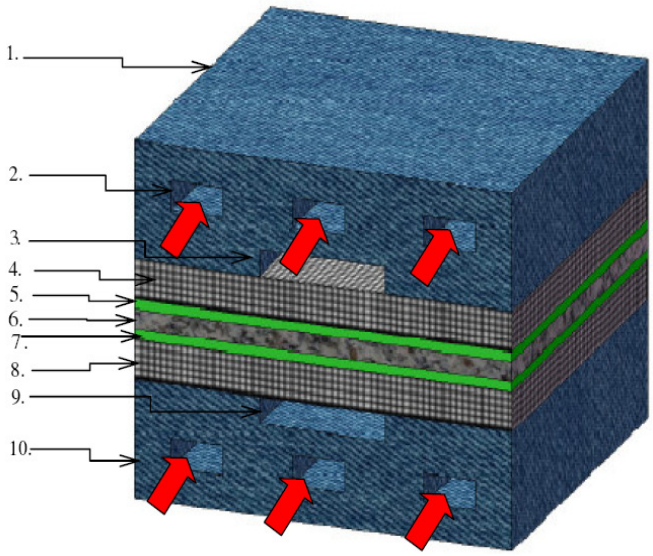

1. Anode-side bipolar plate
2. Cooling channel
3. Hydrogen fuel channel
4. Anode GDL
5. Anode catalyst layer
6. Membrane
7. Cathode catalyst layer
8. Cathode GDL
9. Air gas channel
10. Cathode-side bipolar plate

Figure 1. 3-D schematic of the PEM fuel cell with cooling channels on bipolar plates.

The Dynamic-Q optimisation algorithm [16] is employed as the optimisation search scheme. The optimisation algorithm is expected to ensure robust optimal values for the factors investigated in this study.

Governing Equations

The conservation equations of mass, momentum, species, proton, electron and energy are presented below, viz:

Continuity equation:

$$\nabla \cdot (\rho \mathbf{u}) = 0 \tag{1}$$

Momentum:

$$\frac{1}{\varepsilon^2}\nabla \cdot (\rho \mathbf{u}\mathbf{u}) = -\nabla p + \nabla \cdot \tau + S_u \tag{2}$$

Species:

$$\nabla \cdot (\mathbf{u} C_k) = \nabla \cdot (D_k^{eff} \nabla C_k) + S_k \tag{3}$$

Proton:

$$\nabla \cdot (\kappa^{eff} \nabla \Phi_e) + S_\Phi = 0 \tag{4}$$

Electron:

$$\nabla \cdot (\sigma_s^{eff} \nabla \Phi_s) + S_\Phi = 0 \tag{5}$$

Energy:

$$\nabla \cdot (\rho c_p \mathbf{u} T) = \nabla \cdot (k^{eff} \nabla T) + S_T \tag{6}$$

The energy source term, S_T, depicts the sum of the reversible heat release and the irreversible heat generation. In the catalyst layer, the reversible and irreversible reaction heats as well as latent heat of water phase change are considered; for the membrane, ohm heating of current due to large resistance of the membrane is also considered. Other source terms for the equations above used in the model were taken from Dutta *et al.* [17].The transfer current densities at the anode and the cathode are calculated using the Butler-Volmer equation [18]:

$$i_o = i_{o,ref}\left\{\exp\left[\frac{\alpha_{an} nF}{RT}\eta\right] - \exp\left[\frac{-\alpha_{cat} nF}{RT}\eta\right]\right\} \tag{7}$$

where η is the overpotential and defined as,

$$\eta = (\Phi_s - \Phi_e) - E_{ocv} \tag{8}$$

F is the Faraday constant, α_{an} and α_{cat} represents the experimental anodic and cathodic transfer coefficients, respectively; and R is the universal gas constant.

The effective diffusivity ($D_{i,eff}$) for the gas-phase flow in porous media can be written as:

$$D_{i,eff} = D\frac{\varepsilon}{\tau} \tag{9}$$

The quantity (τ = tortuosity) is usually estimated through experiment. Therefore, it is conventionally correlated in fuel cell studies using the Bruggeman correlation [19]. This correlation assumes τ is proportional to $\varepsilon^{-0.5}$ resulting in the simpler expression [19]:

$$D_{i,eff} = D\varepsilon^{1.5} \tag{10}$$

The porosity correlation is used to account for geometric constraints of the porous media.

The Reynolds number was defined as [20]:

$$\mathrm{Re} = \dot{m}D/(\mu A) \tag{11}$$

Numerical Procedure

The model equations were solved using a finite-volume computational fluid dynamics code FLUENT [21] with GAMBIT® (2.4.6) as a pre-processor. The CFD code has an add-on package for fuel cells, which has the requirements for the source terms for species transport equations, heat sources and liquid water formations. The domain was discretized using a second-order discretization scheme. The pressure-velocity coupling was performed with the SIMPLE algorithm [22] for convection-diffusion analysis. Numerical convergence was obtained at each test condition when the ratio of the residual source (mass, momentum and species) to the maximum flux across a control surface was less than 10^{-7}. Table 2 shows the dimensions of the cooling channels used for initial numerical investigation.

Table 2: Dimension of the cooling channels investigated for initial simulations.

Test Case	W(mm)	H(mm)	L(mm)	$\alpha(=H/W)$
1	0.8	1.5	120	1.875
2	1.2	3.0	120	2.500
3	1.6	4.5	120	2.813

MATHEMATICAL OPTIMISATION ALGORITHM

The Dynamic-Q optimization algorithm [16] was used in this study. The algorithm is a robust multidimensional gradient based optimization algorithm which does not require an explicit line search and it is ideally robust for cases where the function evaluations are computationally expensive. The algorithm applies the dynamic trajectory LFOPC (Leapfrog Optimisation Program for Constrained Problems) which is adapted to handle constrained problems through approximate penalty function formulation [16]. This dynamic approach is applied to successive quadratic approximations of the actual optimization problem. The successive sub-problems are formed at successive design points by constructing spherically quadratic approximations which are used to approximate the objective functions or constraints (or both) if they are not analytically given or very expensive to compute numerically [23,24]. The use of spherically quadratic approximation in the Dynamic-Q algorithm offers a competitive advantage when compared with other algorithm in term of the computational and storage requirements [23]. The storage savings becomes highly significant when the number of variables becomes large. Therefore, this particular strength of the Dynamic-Q method makes it well suited for optimisation of engineering problems with large number of variables and it has been used to successfully solve a large variety of engineering problems [25-27].

OPTIMISATION PROBLEM FORMULATION

The optimization problem was tailored towards finding the best operating design parameters which will give the best performance for the PEM fuel cell. The design variables which greatly affect the performance of the PEM fuel cell especially at high operating temperature are the air stoichiometry ratio, relative humidity (RH), aspect ratio of the cooling channels. The objective function here is the maximised current density of the fuel cell system at optimised operating factors (stoichiometry ratio, relative humidity and cooling channel aspect ratio) at fixed Reynolds number of the coolant and pressure drop of less than 3 atm.

The objective function for the optimization can be written mathematically as,

$$I_{\max} = f(\lambda_{opt}, RH_{opt}, H/W_{opt}, Re) \tag{12}$$

where $I_{\max}$ is the maximized current density output for the optimized design variables.

Design Variables Constraints

The following constraints were used for the optimization:

$$1 \le \lambda \le 5 \tag{13}$$

$$0.2 \le RH \le 0.5 \tag{14}$$

$$1.5 \le \frac{H}{W} \le 3.5 \tag{15}$$

Optimisation Procedure

The optimization problem defined in Section above was solved by coupling the Dynamic-Q optimization algorithm with computational fluid dynamics code FLUENT [21] and grid generation (GAMBIT [28]) code in a MATLAB [29] environment. To ensure that the converged solution obtained is indeed the global minimum, a multi-starting guess approach was employed.

RESULTS AND DISCUSSION

Model Validation

The validation of physical and numerical models is very important; hence comparison with some experimental data is

highly desirable. For fuel cell performance description, the polarisation curve or voltage-current (*IV*) curve is one of the most important final outcomes of numerical simulation and is widely used for validation purposes [18]. The simulation results for the base case operating conditions were verified against measurements of Wang *et al.* [30]. The computed polarisation curve shown in Figure 2 is in good agreement with the experimental curves especially in the low load region. However, the model current density in the high mass transport limited region (> 1.5 A/cm^2) is higher than the experimental values. This observation is common in models where the effect of reduced oxygen transport due to water flooding at the cathode at higher current density cannot be properly accounted for [31].

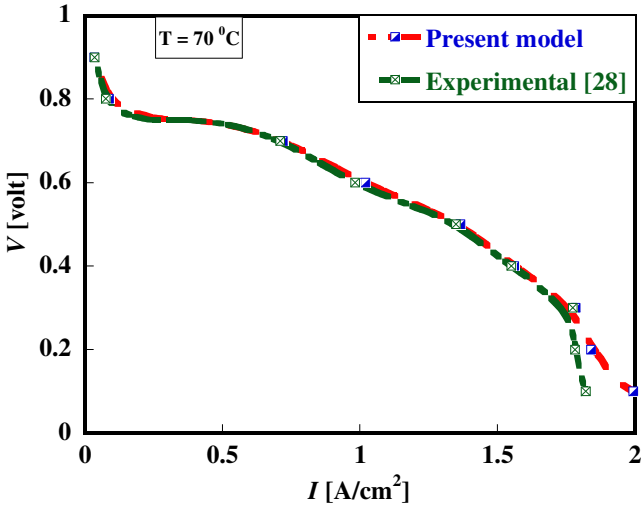

Figure 2. Comparison of numerical model prediction and experimental polarisation curves at base condition.

Results of Operating Parameters

Fig. 3 shows the polarisation curve at varying stoichiometry number for a constant temperature (70 ^{0}C) and pressure (P = 3 bar). For a low stoichiometry number, the removal of the cathode outlet flow decreases, thereby keeping the water concentration in the membrane layer increasing. This result in lower membrane resistance and the resulting ohmic over-potential become lower thereby leading to improved cell performance. However, at higher current density of the fuel cell, the low stoichiometry number adversely affects the cathode over-potential due to excessive resident water in the catalyst.

Fig. 4 shows the influence of relative humidity at the cathode inlet on the fuel cell output voltage. As the relative humidity at cathode inlet increases, air transport to the catalyst is hindered resulting in increasing cathode over-potential especially at high operating current density of the fuel cell system. This condition hinders optimal fuel cell performance.

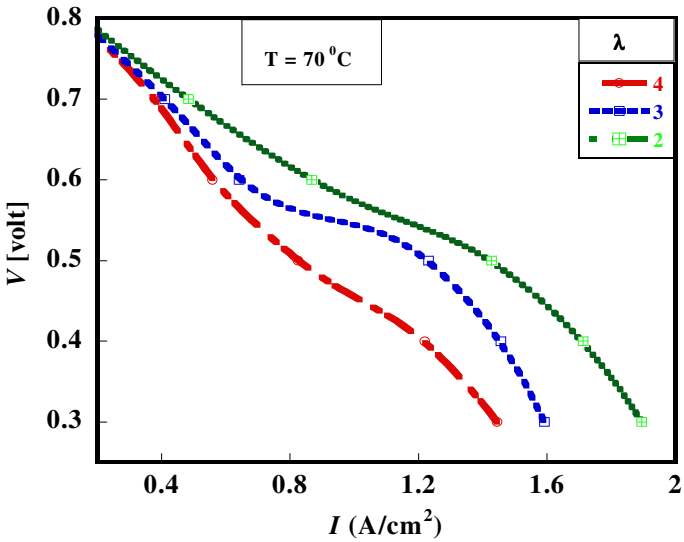

Figure 3. *I-V* curve at varying stoichiometry number. P = 3.0 bar and Re = 500.

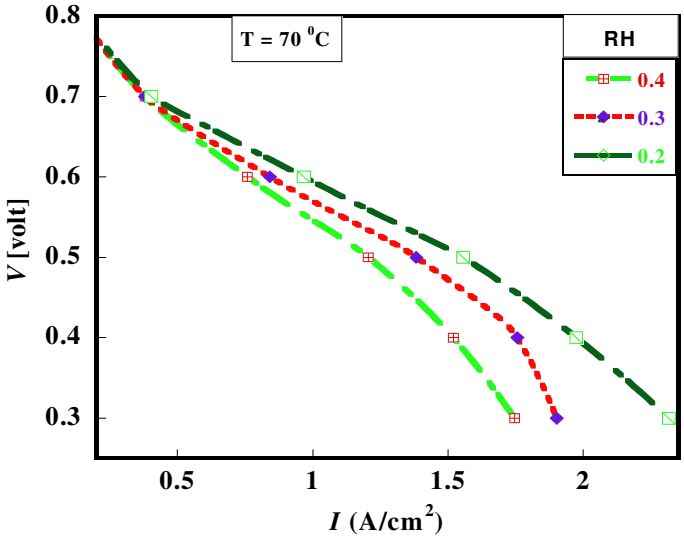

Figure 4. *I-V* curve at varying relative humidity (RH). P = 3.0 bar and Re = 500.

Fig. 5 shows the fuel cell performance at different aspect ratio of the cooling channels for a Reynolds number of 500. The result shows that fuel cell performance increases as the aspect ratio of the cooling channels increases at operating temperature of 70 ^{0}C until an optimal aspect ratio of $\approx 3.0mm$. Beyond the aspect ratio of about 3.0, the cell performance starts depleting. This is likely due to excessive water accumulation in the fuel cell system hindering system performance. This result shows that such optimal channel aspect ratio exist that optimises the fuel cell performance in term of current density.

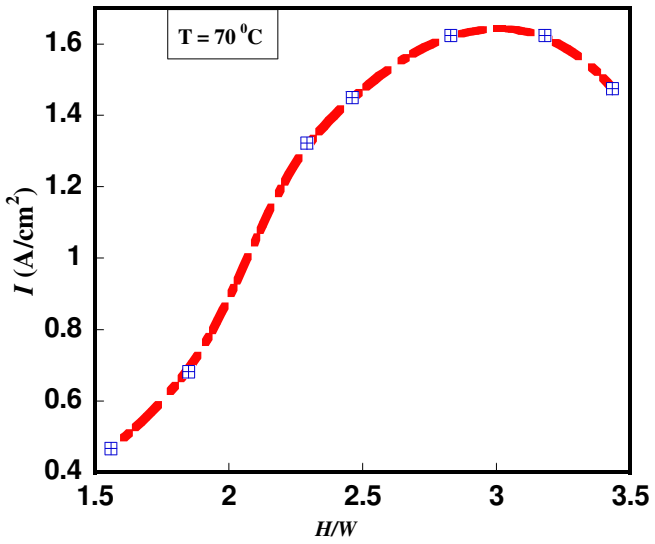

Figure 5. The cell current density at different aspect ratio at a cell potential of 0.3 V and a fixed Reynolds number of 500.

Fig. 6 shows the *IV* curve for the 3 cases (Table 2) of cooling channel aspect ratio investigated at the base operating condition of the fuel cell. It is observed that fuel cell performance increases with increasing cooling channel aspect ratio at cell operating temperature of 70 °C. This increase in performance is likely due to increasing species transport to the reaction site of the fuel cell system and subsequently aiding electrochemical reaction.

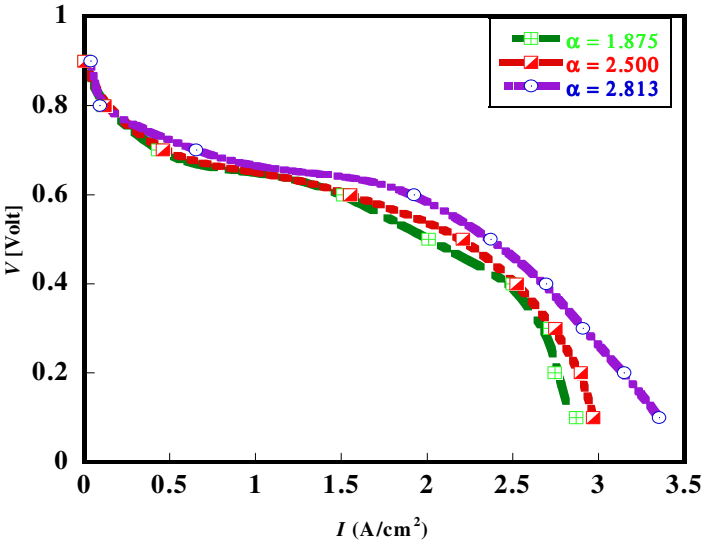

Figure 6. Current density at three cases of channel aspect ratio and Re = 500.

Optimisation Results

The results on the effect of stoichiometry ratio, relative humidity and cooling channel aspect ratio on the output current density suggests the possibility of optimal combination of these parameters for improved performance of the PEM fuel cell at increase temperature beyond the critical operating temperature typical of low temperature PEM fuel cell. These factors are mutually dependent and also affect the rate of membrane hydration which determines reaction and transport characteristics in the fuel cell system. The optimal values obtained for these factors (stoichiometry ratio, relative humidity and cooling channel aspect ratio) are combined with varying cell operating temperatures to examine the fuel cell performance especially when operation at higher temperatures (HT) is desired. It is well known that operating PEM fuel cell at higher operating temperatures eliminates some of the complications hindering improved performance. An intermediate HT-PEM (100 - 150 °C) operating situation is investigated. Table 3 presents the optimal values for the optimised parameters.

The maximised fuel cell performance for the combination of these optimal parameters (in Table 3) at higher cell operating temperatures of fuel cell was investigated. Table 4 shows the polarisation data based on the optimal design parameters for the different operating fuel cell voltages and temperatures. The results presented in table 4 shows that there is improvement in cell performance at different cell voltages considered with increasing cell operating temperature. Higher performance was obtained at low cell operating voltages compared to higher cell voltages at different temperatures ranges. Increase in cell current density difference was more prominent between the temperature range of 120 °C and 130 °C, but at temperature of 150 °C the performance was not very significant. When the operation was conducted beyond the 150 °C, the temperature increase became insignificant. This is most likely due to high level of membrane dehydration beyond this temperature (150 °C) level.

Table 3: Values of optimised parameters.

Model parameters	Optimised values (0.3 V)
λ	4.246
RH	0.323
H/W	3.211

Table 4: Polarisation data at optimised conditions and varying cell operating temperatures at fixed coolant Re = 500.

Cell Voltage (V)	Current(A/cm^2) (T = 120 °C)	Current(A/cm^2) (T = 130 °C)	Current(A/cm^2) (T = 150 °C)
0.7	3.9511	4.6332	4.8512
0.6	5.2333	5.9432	6.3447
0.5	5.7432	6.2448	6.9234
0.3	6.5222	8.7431	9.2281

CONCLUSION

A numerical and optimisation approaches aimed at improving PEM fuel cell performance at elevated operating temperatures (> 80 °C) has been presented. The numerical results show that operating parameters such as stoichiometry ratio, relative humidity and cooling channel aspect ratio has significant effect on fuel cell performance primarily by determining the level of membrane dehydration of the PEM fuel cell. Optimal values of stoichiometry ratio, relative humidity and cooling channel aspect ratios were obtained by integrating a direct problem solver with an optimiser (Dynamic-Q). For the PEM fuel cell model considered in this work, fuel cell performance is considerably enhanced by a combination of parameters, such as stoichiometry ratio, relative humidity and cooling channel aspect ratio. Performance is well enhanced at temperature between 120 °C and 130 °C. The performance increment declines gradually from 130 °C to 150 °C. It should be noted that beyond the 150 °C, there is no significant increase in cell performance. In summary, the result of this study shows the possibility of operating PEM fuel cell beyond the critical temperature ($\leq$80 °C) using the combined optimal of stoichiometry ratio, relative humidity and cooling channel geometry without the need for special temperature resistant materials for the PEM fuel cell. This work can easily be extended to varying cooling channel geometries for enhanced PEM fuel cell performance.

ACKNOWLEDGEMENT

This work was supported by the University of Pretoria, NRF, TESP, EEDSM Hub, CSIR, and the Solar Hub of the University of Pretoria and Stellenbosch University.

REFERENCES

[1] Siegel N.P., Ellis M.W., Nelson D.J., von Spakovsky M.R., Single domain PEMFC model based on agglomerate catalyst geometry, *J. Power Sources* 115 (2003) 81-89.

[2] Faghri A., Guo Z., Challenges and opportunities of thermal management issues related to fuel cell technology and modelling, *Int. J. Heat Mass Transfer* 48 (2005) 3891-3920.

[3] Li Q.F., He R.H., Jensen J.O., Bjerrum N.J, Approaches and recent development of polymer electrolyte membranes for fuel cells operating above 100 °C, *Chem. Mater.* 15 (2003) 4896-4915.

[4] Zhang J.L., Xie Z., Zhang J.J., Tanga Y.H., Song C.J., Navessin T., Shi Z.Q., Song D.T., Wang H.J., Wilkinson D.P., Liu Z.S., Holdcroft S., High temperature fuel cells, *J. Power Sources* 160 (2006) 872-891.

[5] Shao Y.Y., Yin G.P, Wang Z.B, Gao Y.Z., Proton exchange membrane fuel cell from low temperature to high temperature: material challenges, *J. Power Sources* 167 (2007) 235-242.

[6] Li Q.F., Rudbeck H.C., Chromik A., Jensen J.O., Pan C., Steenberg T., Calverley M., Bjerrum N.J., Kerres J., Properties, degradation and high temperature fuel cell test of different PBI and PBI blend membranes, *J. Membr. Sci*. 347 (2010) 260-270.

[7] Yuan J., Faghiri M., Sunden B., On heat and mass transfer phenomena in PEMFC and SOFC and modelling approaches: In Transport Phenomena in Fuel Cells, B. Sunden & M. Faghiri (eds), 133-174, WIT Press, 2005.

[8] Zhang Y.J., Ouyang M.G., Luo J.X., Zhang Z., Wang Y.J., Mathematical modeling of vehicle fuel cell power system thermal management, *SAE Pap.* 1 (2003) 11-46.

[9] Andrew R., Li X.G., Mathematical modeling of proton exchange membrane fuel Cells, *J. Power Sources* 102 (2001) 82-96.

[10] Yu X., Zhou B., Sobiesiak A., Water and thermal management for Ballard PEM fuel cell stack, *J. Power Sources* 147 (2005) 184-195.

[11] Coppo M., Siegel N.P., von Spakovsky M.R., On the influence of temperature on PEM fuel cell operation, *J. Power Sources* 159 (2006) 560-569.

[12] Yan W.-M., Chen F., Wu H.-Y., Soong C.-Y., Chu H.-S., Analysis of thermal and water management with temperature-dependent diffusion effects in membrane of proton exchange membrane fuel cell, *J. Power Sources* 129 (2004) 127-137.

[13] Shimpalee S., Dutta S., Numerical prediction of temperature distribution in PEM fuel cells, *Numerical Heat Transfer (Part A)* 38 (2000) 111-128.

[14] Obayopo S.O., Bello-Ochende T., Meyer J.P., Three-dimensional optimisation of a fuel gas channel of a PEM fuel cell for maximum current density, *International Journal of Energy Research* 2011;DOI:10.1002/er.1935.

[15] Ju H., Meng H., Wang C.Y., A single-phase, non-isothermal model for PEM fuel Fuels, *Int. J. Heat Mass Transfer* 48 (2005) 1303-1315.

[16] Snyman J.A., Practical mathematical optimization: an introduction to basic optimization theory and classical and new gradient-based algorithm, New York: Springer; 2005.

[17] Dutta S., Shimpalee S., Van Zee J.W., Numerical prediction of mass exchange between cathode and anode channels in a PEM fuel cell, *Int. J. Heat Mass Transfer* 44 (2001) 2029-2042.

[18] Cheng C.H., Lin H.H., Lai G., Design for geometric parameters of PEM fuel cell by integrating computational fluid dynamics code with optimisation method, *J. Power Sources* 165 (2007) 803-813.

[19] Mench MM. Fuel cell engines. New Jersey: John Wiley & Sons; 2008.

[20] Tanda G. Heat transfer and pressure drop in a rectangular channel with diamond-shaped elements. Int J Heat Mass Transfer 2001;44:3529-41.

[21] Ansys *Fluent® 12.0 Users Guide Documentation*, Ansys Inc., Southpointe, SAS; 2009.

[22] Pantakar S.V., Numerical heat transfer and fluid flow, New York: Hemisphere Publishing Corp.;1980.

[23] Snyman J.A., Hay A.M., The DYNAMIC-Q optimization method: an alternativeto SQP?'. *Computer and Mathematics with Applications* 44 (2002) 1589-1598.
[24] Bello-Ochende T., Meyer J.P., Ighalo F.U., Combined numerical optimization andconstructal theory for the design of micro-channel heat sinks, *Numerical Heat Transfer, Application Part A* 58 (2010) 882-899.
[25] Ighalo F.U., Bello-Ochende T., Meyer J.P., Mathematical optimization: application to the design of optimal micro-channel heat sinks, *Engenharia Termica* 2009;8(1):58-64.
[26] Le Roux W.G., Bello-Ochende T., Meyer J.P., Operating conditions of an open and direct solar thermal Brayton cycle with optimised cavity receiver and recuperator, *Energy* 36 (2011) 6027-6036.
[27] Le Roux W.G., Bello-Ochende T., Meyer J.P. , Thermodynamic optimization of an integrated design of a small-scale solar thermal Brayton cycle, *Int J Energy Res* (2011); DOI: 10.1002/ER.1859.
[28] Fluent Inc., Gambit Version 6 Manuals, 2001.
[29] The Mathworks Inc., MATLAB & Simulink release notes for R2008a, 2008.
[30] Wang L., Husar A., Zhou T., Liu H., A parametric study of PEM fuel cell performances, *Int. J. Hydrogen Energy* 28 (2003) 1263-1272.
[31] T. Berning, N. Djilali, J., A 3D multiphase, multicomponent model of the cathode and anode of a PEM fuel cell, *Electrochem. Soc.* 150(12) (2003) A1598-A1607.